DNA Nanostructures

DOI: 10.1002/anie.201007403

Chiral Metal–DNA Four-Arm Junctions and Metalated Nanotubular Structures**

*Hua Yang, Florian Altvater, A. Dowine de Bruijn, Christopher K. McLaughlin, Pik Kwan Lo, and Hanadi F. Sleiman**

DNA is a promising template for the programmable assembly of nanostructures.[1] A number of construction strategies have been developed, such as the weaving together of many DNA strands into "tiles"[2] or the stapling of a long DNA strand into "origami" assemblies.[3] These approaches use DNA as the only information source for organization and result in DNA-dense, large, and rigid nanostructures. An interesting alternative is the introduction of synthetic molecules to create DNA assemblies with new structures and functions.[4–6] The use of organic or inorganic molecules as junctions can eliminate the need to interweave DNA strands for structural definition and thus results in "DNA-economical" structures with smaller sizes and increased dynamic character. Transition-metal junctions are especially useful, because they can impart functional advantages, such as photophysical, redox, catalytic, and magnetic properties, as well as enhanced stability to DNA nanostructures.[5,6]

Because of their diverse coordination geometries, transition metals may also have key *structural* advantages for DNA nanoconstruction. They can lead to junction architectures that are inaccessible with DNA alone and may be able to mediate the transfer of chirality from the DNA double helix to the junction itself. Such chirality transfer is particularly desirable, as many DNA junctions are intrinsically chiral because of sequence and groove asymmetry, and their assembly can lead to diastereomeric mixtures. Control of the chirality of these junctions can result in stereospecific, higher-yielding DNA-nanostructure syntheses and more specific interactions with other biological molecules.[7]

Herein we describe a DNA-templated method for the formation of a chiral metal–DNA junction containing a single copper(I)–bisphenanthroline unit at its central point and four single-stranded DNA arms of different sequences. This structure is the simplest, most compact four-arm junction derived from DNA and would be difficult to access without the mediation of the transition metal. The design, evolution, and optimization of the metal–ligand complex for efficient chirality transfer from DNA is reported. From this structure, we then constructed metal–DNA triangular rungs and formed the first metal–DNA nanotubular structures.

In our approach to the construction of chiral junctions with four different arms, we use two DNA strands, **D1** and **D2**, each modified in the middle of the 20-base sequence with a diphenylphenanthroline (dpp) ligand (Figure 1 a). A template strand **T** is used to bring **D1** and **D2** together. After the hybridization of **D1** and **D2** with **T**, the two dpp ligands are in close proximity, and the addition of copper ions results in the formation of a $Cu(dpp)_2$ complex that links **D1** and **D2** together.

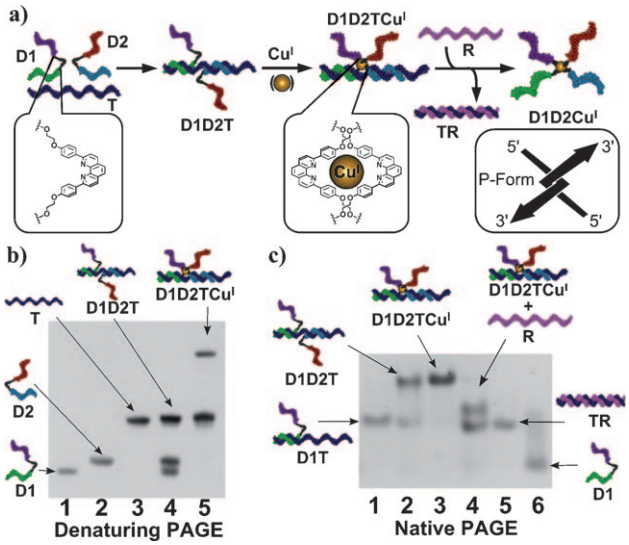

Figure 1. Templated synthesis of a DNA–metal junction with four different single-stranded arms. a) The template strand, **T**, hybridizes with **D1** and **D2**. Cu^I coordination links **D1** and **D2**, and then **T** can be removed by its complementary strand **R** to generate the single-stranded junction **D1D2Cu^I**. b) Denaturing PAGE (12%, 4 M urea) analysis of Cu^I coordination to the hybridized structure: **D1** (lane 1) and **D2** (lane 2) on template **T** (lane 3). **D1D2T** completely denatured (lane 4); however, its Cu^I complex denatured to **T** and the metal-connected structure **D1D2Cu^I**. c) Native PAGE (12%) analysis of the hybridization of **D1** and **D2** with template **T** (lane 2), Cu^I complexation (lane 3), and the displacement of **T** with its complementary strand **R** to generate **TR** and the fully single stranded junction **D1D2Cu^I** (lane 4).

Before the addition of copper ions, native polyacrylamide gel (PAGE) analysis showed efficient hybridization of the three components **D1**, **D2**, and **T** to form one structure (Figure 1 c, lane 2). When placed on a denaturing PAGE gel, this structure disassembled into its three components (Figure 1 b, lane 4). After the addition of copper(I) ([Cu-

[*] Dr. H. Yang, F. Altvater, A. D. de Bruijn, C. K. McLaughlin, P. K. Lo, Prof. H. F. Sleiman
Department of Chemistry, McGill University
801 Sherbrooke Street West, Montreal, Quebec H3A 2K6 (Canada)
Fax: (+1) 514-398-3797
E-mail: hanadi.sleiman@mcgill.ca

[**] We acknowledge the NSERC, the CSACS, and the CIFAR. H.F.S. is a Cottrell Scholar of the Research Corporation.

Supporting information for this article is available on the WWW under http://dx.doi.org/10.1002/anie.201007403.

$(CH_3CN)_4]^+$, 1.2 equiv) to the **D1D2T** junction, native PAGE showed that the hybridization of the three components into a single structure **D1D2TCu^I** was preserved (Figure 1c, lane 3). Importantly, denaturing PAGE showed two bands, one corresponding to the template strand **T**, and a lower-mobility band assigned to the metal complex **D1D2Cu^I** (Figure 1b, lane 5). No bands corresponding to **D1** or **D2** were detected, a result consistent with quantitative metalation of these two strands to give **D1D2Cu^I**, which resists denaturation. We verified that this product was the heterodimer **D1D2Cu^I** (rather than a homodimer) by generating the two homodimers **(D1)$_2$Cu^I** and **(D2)$_2$Cu^I** through copper complexation of **D1** and **D2** without the template strand. The homodimers were formed in lower yield and could be distinguished from the heterodimer **D1D2Cu^I** by comparing their mobility on denaturing PAGE (see Figures S4 and S6 in the Supporting Information).

In **D1D2TCu^I**, the template **T** has a five-base overhang, which makes it removable from the **D1D2Cu^I** complex by the addition of a completely complementary strand **R** (Figure 1a). When **R** was added to **D1D2TCu^I**, two bands were observed on the native PAGE gel (Figure 1c): one that had the same mobility as **TR**, and one of lower mobility that was assigned as **D1D2Cu^I** (lane 4). This result indicated the formation of **D1D2Cu^I** by the DNA-templated organization of its two components. The **D1D2Cu^I** assembly is a four-arm junction with a metal complex at the vertex and four different DNA single-stranded arms. Such junctions are small, information-dense building blocks that provide a number of possibilities for 2D and 3D construction. Their direct synthesis would be challenging, as the independent growth of four different DNA strands from a central branch point would require many orthogonal protection/deprotection steps.[8] Thus, the use of metal complexes in the construction of DNA structures can be very advantageous.

We then turned our attention to chirality transfer from the DNA double helix to these junctions. In our initial system with template **T1**, the sequences complementary to one 10 base arm of **D1** and one 10 base arm of **D2** are directly adjacent to each other with no unhybridized bases on the template strand **T1** (Figure 2a). When a metal ion coordinates in this environment, either right-handed (*P*) or left-handed (*M*) helicity can be adopted. If one of these orientations is preferred, a signal is expected in the circular dichroism (CD) spectrum in the 300–400 nm region, where the ligand absorbs.[6,9] We had previously observed this signal for a Cu(dpp)$_2$ unit residing at the end of a DNA duplex (**D3D4Cu^I**, Figure 2e).[6] However, although the denaturing gel demonstrated efficient formation of the junction **D1D2Cu^I** with **T1** as the template (see Figure S2), no CD signal was observed in this region (Figure 2a). Thus, a mixture of the *P* and *M* configurations of the Cu(dpp)$_2$ complex was formed. Molecular modeling indicated that the metal center was forced out of contact with the DNA-helix environment

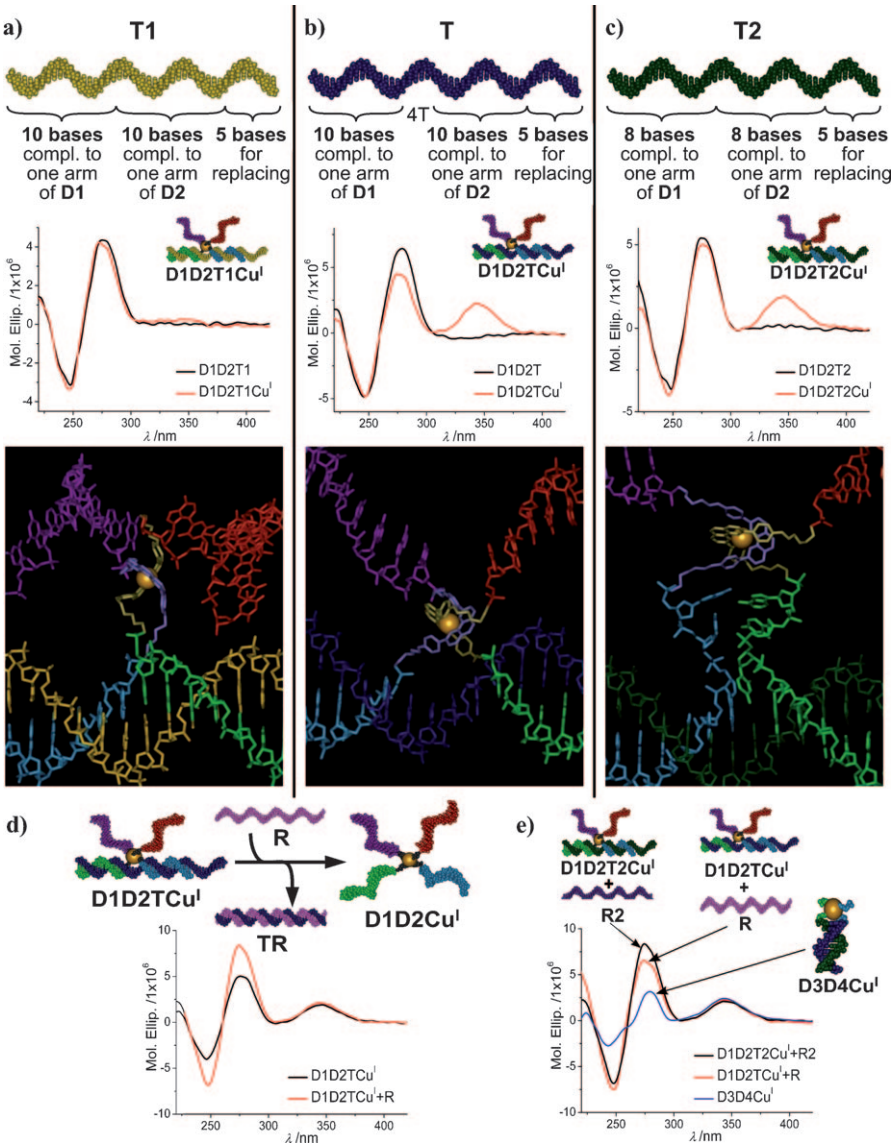

Figure 2. Formation of chiral four-arm DNA–metal junctions. a–c) Design of the templates **T1**, **T**, and **T2**, molecular modeling of **D1D2T1Cu^I**, **D1D2TCu^I**, and **D1D2T2Cu^I**, and CD spectra in which an induced band at 300–400 nm indicates the chirality of the metal complex. d) The CD spectrum after the addition of the removing strand **R** to **D1D2TCu^I** shows that the signal for the metal center is retained. e) Quantitative comparison of the chirality of the three metalated structures **D1D2T2Cu^I** + **R2**, **D1D2TCu^I** + **R**, and **D3D4Cu^I** (same concentration in dpp).

because of the lack of a spacer between the two strands **D1** and **D2**, and thus the chirality of the DNA helix was not transferred to the metal complex (Figure 2a).

To bring the dpp ligands closer to the DNA environment and enable transfer of chirality to the metal complex, we redesigned the template **T** with a spacer of four thymine bases to separate the sequences complementary to **D1** and **D2**. We hoped that this design would still lead to formation of the $Cu(dpp)_2$ complex but enable the complex to form closer to the chiral DNA environment and would thus favor chirality transfer through noncovalent contacts (Figure 2b; see the molecular model). In this case, PAGE (denaturing and native) confirmed the formation of **D1D2TCu^{I}** (Figure 1b,c), and the CD spectrum showed a large positive peak at 345 nm (Figure 2b) indicative of a *P*-form (right-handed-helical) metal complex. We confirmed the stoichiometry of the metal complex, with a single metal center at the **D1D2** junction, by titrating **D1D2T** with Cu^{I} and monitoring the CD signal at 345 nm (see Figure S7). These results indicate that by causing the metal complex to form in close proximity to the DNA double helix, a chiral junction can be formed with four different arms and a metal complex at the center.

In earlier studies, we found that the chirality of the DNA double helix could be transferred to metal complexes formed at the duplex end.[6] We thus designed a third template strand **T2**, with a sequence complementary to only eight bases each of **D1** and **D2**. Upon hybridization, **D1** and **D2** would still have two free bases between their dpp ligands and the template region (Figure 2c). Molecular modeling showed that the ligands may engage in π–π interactions with the free DNA bases that are fixed along the preorganized DNA duplex. Such interactions could potentially result in chirality transfer from the DNA to the metal complex upon the addition of Cu^{I}. CD analysis of the **D1D2T2Cu^{I}** complex also revealed the formation of the *P*-form complex (Figure 2c). This study demonstrates the importance of the interaction between the target compound and the DNA environment for the synthesis of a chiral junction, and shows how fine-tuning of the DNA structure can result in very different stereochemical outcomes.

Importantly, the chirality of this junction was retained after the removal of the template strand. In the CD spectrum (Figure 2d), the signal at 345 nm remained unmodified, whereas the signal at 200–300 nm increased in intensity, which is consistent with the increased amount of DNA in the sample. The lack of change observed in the CD spectrum of **D1D2Cu^{I}** over three days indicates the stability of this chiral metal junction (see Figure S11).

To estimate the extent of chirality transfer to the junction, we compared the junctions made with **T** and **T2** with our previously developed structure **D3D4Cu^{I}**, in which the $Cu(dpp)_2$ unit is at the end of a DNA duplex (Figure 2e). At the same concentration of dpp, **D1D2T2Cu^{I}** + **R2**, **D1D2TCu^{I}** + **R**, and **D3D4Cu^{I}** gave very similar CD signals at 345 nm. Thus, although the *P*-to-*M* ratio cannot be determined yet, we conclude that this chirality transfer is efficient in all cases, since the different approaches used (see also below) produce complexes with similar *ee* values.

The orientation of the arms of these chiral four-arm junctions can mediate the assembly of higher-order DNA structures. We used these building blocks to generate metal–DNA nanotubular assemblies. To this end, we designed triangular "rungs" consisting of three chiral junctions: **C1Cu^{I}**, **C2Cu^{I}**, and **C3Cu^{I}** (Figure 3a). Each DNA arm for cyclization is 15 bases long: 5 bases to provide flexibility for efficient cyclization, and 10 to hybridize with other arms (Figure 3a).

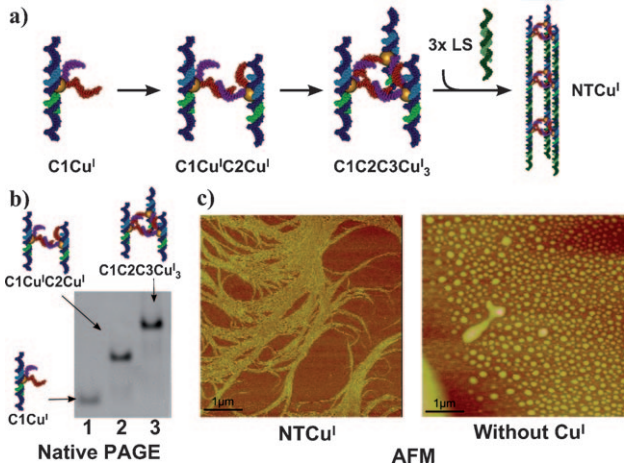

Figure 3. Assembly of a metal–DNA nanotubular structure. a) Three chiral four-arm junctions (**C1Cu^{I}**, **C2Cu^{I}**, and **C3Cu^{I}**) hybridize to form a cyclic structure. Such cyclic structures can be connected by linking strands (**LS**) and act as "rungs" on the resulting tubular structure. b) Native PAGE (8%) analysis of the stepwise hybridization of three templated four-arm junctions: lane 1: **C1Cu^{I}**; lane 2: **C1Cu^{I}** + **C2Cu^{I}**; lane 3: **C1C2C3Cu$^{I}_3$**. c) AFM analysis of the metalated nanotubular structure **NTCu^{I}** (left) and the control sample prepared without Cu^{I} (right) on a mica surface under dry conditions.

Template strands (dark blue) rigidify two of the DNA arms attached to the Cu^{I} ions and provide sticky ends above and below the plane of the triangle. All six sticky ends are different; each "rung" contains three sticky ends "pointing up" and three sticky ends "pointing down". If the chirality of the corner units was not controlled, the rung would be a mixture of eight structures with different orientations of the sticky ends (see Figure S14). The rungs would then form ill-defined structures when connected. The use of well-defined chiral junctions can result in a single orientation of the sticky ends in the rung, and nanotubes can form when the rungs are connected. Native PAGE analysis showed the quantitative formation of a trimer structure (Figure 3b). At the same dpp concentration, the triangle corners **C1Cu^{I}**, **C2Cu^{I}**, and **C3Cu^{I}** and the rung **C1C2C3Cu$^{I}_3$** all showed similar CD signal intensities at 300–400 nm (see Figure S17) of a similar magnitude to that observed for **D1D2TCu^{I}**. This result indicates that the chirality of the junctions is sustained in the rung.

Three sets of linking strands (**LS**) were used above and below the plane of the triangular rungs to connect these rungs together and generate elongated structures. We used a hierarchical assembly to facilitate the formation of a linear structure.[10] One set of linking strands has sticky ends 14 bases

long, and the other two sets have 10 base sticky ends. After heating of the DNA strands, the longer sticky ends assemble first during the slow cooling process. The favorable cohesion of the shorter strands follows. Atomic force microscopy (AFM) showed the formation of long one-dimensional structures. Like the nonmetalated nanotubes previously generated in our laboratory,[10] these tubular structures associate with one another on the mica surface under dry conditions with an Mg^{2+} buffer (Figure 3c, left). In contrast, the self-assembly of nonmetalated triangles under the same conditions only gave globular structures (Figure 3c, right).[11] The metal–DNA nanotubular structures hold promise for a number of applications, for example, as templates and catalysts for nanowire growth, well-defined scaffolds for artificial photosynthesis, and carriers for the delivery of bioactive molecules or nanoparticles.[10,12] Their metal centers can impart functionalities, or interact with guests carried by the nanotubes in a similar manner to metalloproteins.[13]

In summary, we have built the first chiral metal–DNA junction with four different single-stranded arms. An external template strand brings together two ligand-modified DNA strands for metal coordination. Upon metalation, a metal–DNA junction with four different arms forms. The template strand can be removed to generate a single-stranded four-arm DNA junction. The metal coordination connects the DNA arms and mediates chirality transfer from the DNA double helix to the junction. This four-arm metal–DNA junction will be important in the area of DNA nanotechnology, as it greatly simplifies the construction of three-dimensional structures and networks. Previously, junctions from DNA could only be created by using multiple DNA strands and cross-over points, which resulted in large, DNA-dense, and stiff structures and a limited ability to control chirality. The chiral junctions described herein can be used to assemble a DNA nanotubular structure with site-specific metalation. The highly dense information content, precise spatial arrangement, and functionality of these four-arm junctions makes them effective building blocks that can be adapted to the construction of a number of different 3D metal–DNA structures and networks.

Received: November 24, 2010
Published online: April 26, 2011

Keywords: chirality · DNA · nanostructures · self-assembly · transition metals

[1] a) C. Lin, H. Yan, *Biochemistry* **2009**, *48*, 1663 – 1674; b) F. A. Aldaye, A. L. Palmer, H. F. Sleiman, *Science* **2008**, *321*, 1795 – 1799; c) N. C. Seeman, *Mol. Biotechnol.* **2007**, *37*, 246 – 257; d) S. Pitchiaya, Y. Krishnan, *Chem. Soc. Rev.* **2006**, *35*, 1111 – 1121; e) K. V. Gothelf, T. H. LaBean, *Org. Biomol. Chem.* **2005**, *3*, 4023 – 4037.

[2] C. Lin, Y. Liu, S. Rinker, H. Yan, *ChemPhysChem* **2006**, *7*, 1641 – 1647, and references therein.

[3] P. W. K. Rothemund, *Nature* **2006**, *440*, 297 – 302.

[4] For selected examples of DNA with organic artificial moieties, see: a) J. Zimmermann, M. P. J. Cebulla, S. Monninghoff, G. von Kiedrowski, *Angew. Chem.* **2008**, *120*, 3682 – 3686; *Angew. Chem. Int. Ed.* **2008**, *47*, 3626 – 3630; b) F. A. Aldaye, H. F. Sleiman, *Angew. Chem.* **2006**, *118*, 2262 – 2267; *Angew. Chem. Int. Ed.* **2006**, *45*, 2204 – 2209; c) L. H. Eckardt, K. Naumann, P. W. Matthias, M. Rein, M. Schweitzer, N. Windhab, G. von Kiedrowski, *Nature* **2002**, *420*, 286.

[5] For selected examples of DNA with inorganic moieties, see: a) G. H. Clever, C. Kaul, T. Carell, *Angew. Chem.* **2007**, *119*, 6340 – 6350; *Angew. Chem. Int. Ed.* **2007**, *46*, 6226 – 6236; b) Y. Miyake, H. Togashi, M. Tashiro, H. Yamaguchi, S. Oda, M. Kudo, Y. Tanaka, Y. Kondo, R. Sawa, T. Fujimoto, T. Machinami, A. Ono, *J. Am. Chem. Soc.* **2006**, *128*, 2172 – 2173; c) K. Tanaka, G. H. Clever, Y. Takezawa, Y. Yamada, C. Kaul, M. Shionoya, T. Carell, *Nat. Nanotechnol.* **2006**, *1*, 190 – 194; d) M. Göritz, R. Kramer, *J. Am. Chem. Soc.* **2005**, *127*, 18016 – 18017; e) D. Mitra, N. Di Cesare, H. F. Sleiman, *Angew. Chem.* **2004**, *116*, 5928 – 5932; *Angew. Chem. Int. Ed.* **2004**, *43*, 5804 – 5808; f) J. S. Choi, C. W. Kang, K. Jung, J. W. Yang, Y.-G. Kim, H. Han, *J. Am. Chem. Soc.* **2004**, *126*, 8606 – 8607; g) K. M. Stewart, L. W. McLaughlin, *J. Am. Chem. Soc.* **2004**, *126*, 2050 – 2057; h) K. V. Gothelf, A. Thomsen, M. Nielsen, E. Clo, R. S. Brown, *J. Am. Chem. Soc.* **2004**, *126*, 1044 – 1046; i) K. Tanaka, A. Tengeiji, T. Kato, N. Toyama, M. Shionoya, *Science* **2003**, *299*, 1212 – 1213; j) E. M. Boon, J. K. Barton, *Curr. Opin. Struct. Biol.* **2002**, *12*, 320 – 329; k) H. Weizman, Y. Tor, *J. Am. Chem. Soc.* **2002**, *124*, 1568 – 1569; l) S. Atwell, E. Meggers, G. Spraggon, P. G. Schultz, *J. Am. Chem. Soc.* **2001**, *123*, 12364 – 12367; m) J. L. Czlapinski, T. L. Sheppard, *J. Am. Chem. Soc.* **2001**, *123*, 8618 – 8619.

[6] a) H. Yang, A. Z. Rys, C. K. McLauglin, H. F. Sleiman, *Angew. Chem.* **2009**, *121*, 10103 – 10107; *Angew. Chem. Int. Ed.* **2009**, *48*, 9919 – 9923; b) H. Yang, C. K. McLaughlin, F. A. Aldaye, G. D. Hamblin, A. Z. Rys, I. Rouiller, H. F. Sleiman, *Nat. Chem.* **2009**, *1*, 390 – 396; c) H. Yang, H. F. Sleiman, *Angew. Chem.* **2008**, *120*, 2477 – 2480; *Angew. Chem. Int. Ed.* **2008**, *47*, 2443 – 2446.

[7] a) Y. He, M. Su, P. Fang, C. Zhang, A. E. Ribbe, W. Jiang, C. Mao, *Angew. Chem.* **2010**, *122*, 760 – 763; *Angew. Chem. Int. Ed.* **2010**, *49*, 748 – 751; b) J. C. Mitchell, J. R. Harris, J. Malo, J. Bath, A. J. Turberfield, *J. Am. Chem. Soc.* **2004**, *126*, 16342 – 16343.

[8] U. Feldkamp, B. Sacca, C. M. Niemeyer, *Angew. Chem.* **2009**, *121*, 6110 – 6114; *Angew. Chem. Int. Ed.* **2009**, *48*, 5996 – 6000, and references therein.

[9] a) G. Baum, E. C. Constable, D. Fenske, C. E. Housecroft, T. Kulke, M. Neuburger, M. Zehnder, *J. Chem. Soc. Dalton Trans.* **2000**, 945 – 959; b) M. Yamamoto, M. Takeuchi, S. Shinkai, *Tetrahedron Lett.* **1998**, *39*, 1189 – 1192; c) C. R. Woods, M. Benaglia, F. Cozzi, J. S. Siegel, *Angew. Chem.* **1996**, *108*, 1977 – 1980; *Angew. Chem. Int. Ed. Engl.* **1996**, *35*, 1830 – 1833.

[10] a) F. A. Aldaye, P. K. Lo, P. Karam, C. K. McLaughlin, G. Cosa, H. F. Sleiman, *Nat. Nanotechnol.* **2009**, *4*, 349 – 352; b) P. K. Lo, P. Karam, F. A. Aldaye, C. K. McLaughlin, G. D. Hamblin, G. Cosa, H. F. Sleiman, *Nat. Chem.* **2010**, *2*, 319 – 328. On the basis of AFM, we cannot rule out the possibility that the nanotubular structures might be cross-linked together.

[11] See the Supporting Information.

[12] a) S. M. Douglas, J. J. Chou, W. M. Shih, *Proc. Natl. Acad. Sci. USA* **2007**, *104*, 6644 – 6648; b) Y. Geng, P. Dalhaimer, S. Cai, R. Tsai, M. Tewari, T. Minko, D. E. Discher, *Nat. Nanotechnol.* **2007**, *2*, 249 – 255; c) H. Yan, S. H. Park, G. Finkelstein, J. H. Reif, T. H. LaBean, *Science* **2003**, *301*, 1882 – 1884.

[13] a) L. Que, W. B. Tolman, *Nature* **2008**, *455*, 333 – 340; b) I. Moura, S. R. Pauleta, J. J. G. Moura, *J. Biol. Inorg. Chem.* **2008**, *13*, 1185 – 1195.

